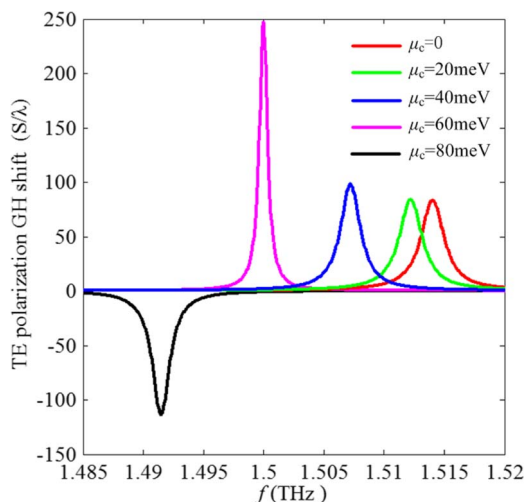


Giant Tunable Goos–Hänchen Shifts Based on Prism/Graphene Structure in Terahertz Wave Region

Volume 6, Number 6, December 2014

Li Jiu-Sheng
Wu Jing-fang
Zhang Le



DOI: 10.1109/JPHOT.2014.2374591
1943-0655 © 2014 IEEE

Giant Tunable Goos–Hänchen Shifts Based on Prism/Graphene Structure in Terahertz Wave Region

Li Jiu-Sheng, Wu Jing-fang, and Zhang Le

Center for Terahertz Research, China Jiliang University, Hangzhou 310018, China

DOI: 10.1109/JPHOT.2014.2374591

1943-0655 © 2014 IEEE. Translations and content mining are permitted for academic research only.

Personal use is also permitted, but republication/redistribution requires IEEE permission.

See http://www.ieee.org/publications_standards/publications/rights/index.html for more information.

Manuscript received August 17, 2014; revised November 13, 2014; accepted November 15, 2014. Date of publication November 26, 2014; date of current version December 17, 2014. This work was supported in part by the National Natural Science Foundation of China under Grant 61379024 and Grant 61131005 and in part by the Zhejiang Province Natural Science Fund for Distinguished Young Scientists under Grant LR12F05001. Corresponding author: L. Jiu-Sheng (e-mail: lijsh2008@126.com).

Abstract: We investigate the giant tunable Goos–Hänchen shifts in prism/graphene structure. It is found that large positive and negative lateral Goos–Hänchen shifts can be easily controlled by adjusting the chemical potential of the graphene, which is modulated by the external applied electric field. By using the stationary-phase method, we theoretically analyze the effect of the external applied electric field on Goos–Hänchen shifts of the proposed prism/graphene structure. Our theoretical study shows that the magnitude of the Goos–Hänchen shift is more than 200 times that of the operating terahertz wavelength. Numerical calculation results further indicate that the present structure has the potential application for the terahertz-wave switch.

Index Terms: Goos–Hänchen shift, graphene, terahertz wave.

1. Introduction

Terahertz (THz) wave ranging from 0.1 THz to 10 THz has been a durative hot topic due to its increasing number of promising and potential application fields over the past few decades. These include biological imaging and sensing, spectroscopy, medical diagnosis, security screening, military detection, radio astronomy, atmospheric studies, communication, etc. [1]–[5]. With the commercialization of terahertz wave source and detector, as an essential part of a terahertz science and technology, terahertz functional components have been paid much attention and their investigations have been dramatically accelerated. Recently, some terahertz filters, modulators, switches, splitters, and polarizers have been reported in the literature [6]–[9]. Relatively, among these investigations, the component available for effectively manipulating terahertz waves is not enough so far. Therefore, the research of the high efficient terahertz functional component becomes indispensable. It is well known that when an electromagnetic wave totally reflected from a planar interface between two different media, a tiny lateral Goos–Hänchen shift between the practical reflect electromagnetic wave and geometric reflect electromagnetic wave takes place [10], [11]. Based on the Goos–Hänchen effect, it is possible to manipulate the reflected terahertz wave beam position. In recent years, a great deal of attention has been given to the development of Goos–Hänchen shift in the microwave, infrared wave and optical regime [12], [13], but very few studies of Goos–Hänchen shift have been conducted in terahertz frequencies region due to

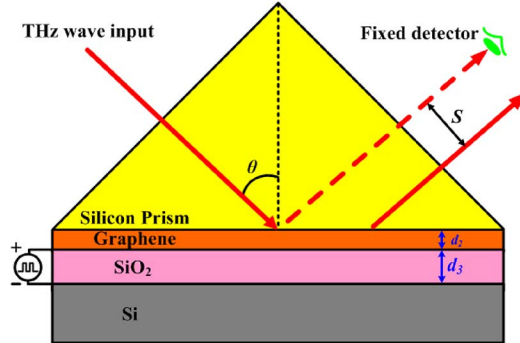


Fig. 1. Schematic of the electrically controlled Goos–Hänchen shift system. (Geometry indicating the Goos–Hänchen shift, a terahertz wave detector is fixed at the extension cord position of dashed line.)

the source and detection problems. More recently, Li *et al.* [14] investigated a Goos–Hänchen shift based on cyclo-olefin copolymer double-prism in terahertz region. However, in all these investigations, the lateral Goos–Hänchen shifts cannot be manipulated for a fixed configuration. In fact, for the applications in terahertz wave components, the manipulation of the Goos–Hänchen shifts of the reflected terahertz wave is vital especially a giant tunable Goos–Hänchen shifts.

To address the performance limitations of existing terahertz wave Goos–Hänchen shifts structure, we investigate a giant tunable Goos–Hänchen shifts scheme using prism/graphene in this letter. This proposal provides a convenient and powerful tool for controlling the lateral Goos–Hänchen shifts of the reflected terahertz wave without changing the proposed prism/graphene configuration, and it also provides a possibility for obtaining the giant negative or positive lateral shift by changing the external controlling electric field. Using the stationary phase method, our theoretical study demonstrates that the magnitude of the Goos–Hänchen shift is more than two-hundred times of the operating wavelength. This configuration have good application prospect because of its simple structure and easy to adjust. Based on this observation, a terahertz switch scheme is presented which, compared to existing terahertz wave switch solutions, has the promise of significant enhancement in switching efficiency over a broad range of terahertz wave frequencies.

2. Device Design and Theory Analysis

In this paper, we assume that the incident terahertz wave is from the silicon prism onto the surface of prism/graphene at the angle (θ) from the normal, as shown in Fig. 1. As shown in Figure, the prism/graphene configuration consists of four layers of materials: silicon prism, graphene, SiO_2 and silicon substrate. In this letter, we suppose that a terahertz wave detector is fixed at the prism external position of the reflected terahertz wave beam (i.e., the extension cord position of dashed line). We consider the Goos–Hänchen shifts (S) of the incident terahertz wave reflected from the interface between prism/graphene interface. For simplicity, we aim at the TE-polarized terahertz wave beam case, for which the electric field is perpendicular to the incident plane.

Firstly, we derive external applied electric field dependent effective permittivity of the graphene. Hence we need to describe the conductivity and permittivity of voltage-biased graphene. Here, we choose a Kubo formula to describe the permittivity of the graphene within terahertz frequencies region. Since the complex conductivity of graphene is composed of intraband and interband terms, it can be written as [15]

$$\sigma(\omega, \mu_c, \Gamma, T) = \sigma_{\text{intra}}(\omega, \mu_c, \Gamma, T) + \sigma_{\text{inter}}(\omega, \mu_c, \Gamma, T) \quad (1)$$

$$\sigma_{\text{intra}}(\omega, \mu_c, \Gamma, T) = -\frac{je^2}{\pi\hbar^2(\omega + j2\Gamma)} \int_0^\infty \xi \left(\frac{\partial f_d(\xi, \mu_c, T)}{\partial \xi} - \frac{\partial f_d(-\xi, \mu_c, T)}{\partial \xi} \right) d\xi \quad (2)$$

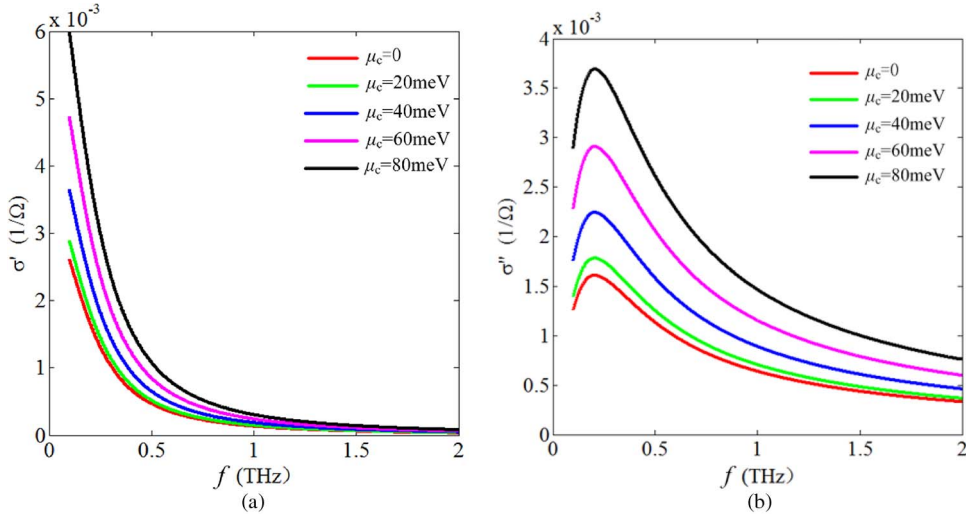


Fig. 2. Conductivity of graphene is plotted versus terahertz wave frequencies for different chemical potential. (a) Real part. (b) Imaginary part.

and

$$\sigma_{\text{inter}}(\omega, \mu_c, \Gamma, T) = \frac{je^2(\omega + j2\Gamma)}{\pi\hbar^2} \left[\int_0^\infty \frac{f_d(-\xi, \mu_c, T) - f_d(\xi, \mu_c, T)}{(\omega + j2\Gamma)^2 - 4\left(\frac{\xi}{\hbar}\right)^2} \right] \quad (3)$$

where $f_d(\xi, \mu_c, T) = (e^{(\xi-\mu_c)/k_B T} + 1)^{-1}$ is the Fermi level, ω is the angular frequency, ξ is the electron kinetic energy, μ_c is the chemical potential which is related to the material doping and bias voltage, Γ is the scattering rate, $\Gamma = 0.43$ meV, T is the absolute room temperature, $T = 300$ K, e is the charge of an electron, \hbar is the reduced Planck's constant, and k_B is the Boltzmann's constant. As we known, in terahertz wave low frequency region, the interband terms of the graphene is very small compared with the intraband terms, so it can be negligible. By solving (1)–(3), we can obtain the expressions for the complex conductivity of the graphene as [16]

$$\sigma \approx \sigma_{\text{intra}} = \sigma'_{\text{intra}} + j\sigma''_{\text{intra}} = \frac{je^2 k_B T}{\pi\hbar^2(\omega + j2\Gamma)} \left[\frac{\mu_c}{k_B T} + 2\ln\left(e^{\frac{\mu_c}{k_B T}} + 1\right) \right]. \quad (4)$$

According to (4), we calculate the frequency characteristic curves versus the conductivity of the graphene for different chemical potential as illustrated in Fig. 2. The relationship between the conductivity and permittivity of graphene is defined as $\varepsilon = \varepsilon' + \varepsilon'' = 1 + i\sigma/(\omega d_2 \varepsilon_0)$. As an example, Fig. 3 shows the frequency characteristic curves versus the graphene permittivity for different chemical potential.

The relationship of electric bias field E_0 and chemical potential μ_c can be given by [17]

$$\frac{2\varepsilon_b E_0}{e} = \frac{2}{\pi\hbar^2 v_F^2} \int_0^\infty \xi [f_d(\xi, \mu_c, T) - f_d(\xi + 2\mu_c, \mu_c, T)] d\xi \quad (5)$$

where ε_b is the dielectric constant of SiO_2 and $\varepsilon_b = 3.9$, v_F is the fermi velocity, and $v_F \approx 1 \times 10^6$ m/s. Fig. 4 illustrates the relation curve of electric bias field E_0 and chemical potential μ_c . From this figure one sees that the chemical potential of the graphene increases as the external applied electric bias field increases.

In this case the reflection coefficient becomes complex and we can write it as $r = |r|\exp(i\varphi_r)$, where φ_r is the phase angle. For the TE-polarized terahertz wave beam the reflection

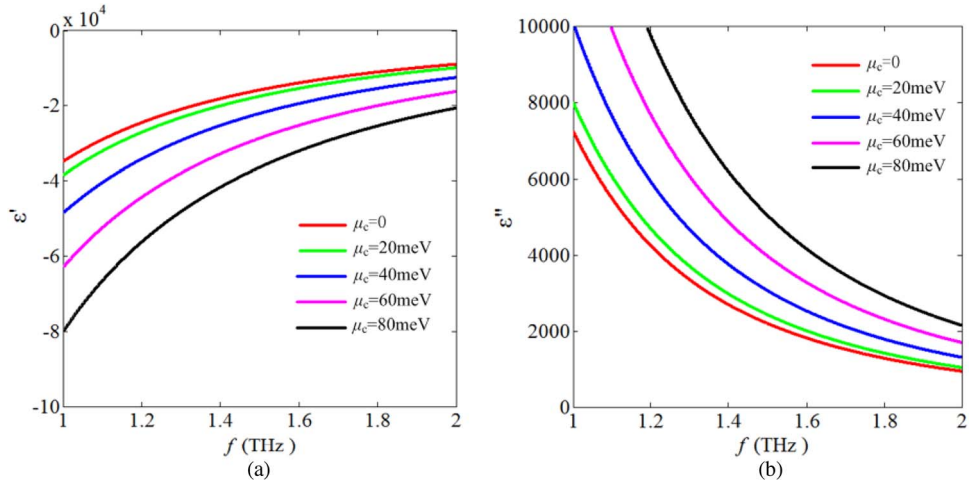


Fig. 3. Permittivity of graphene is plotted versus terahertz wave frequencies for different chemical potential. (a) Real part. (b) Imaginary part.

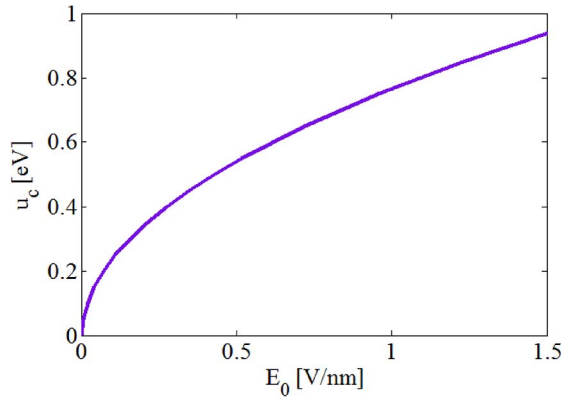


Fig. 4. Relation curve of electric bias field E_0 and chemical potential μ_c .

coefficients (r) of the proposed structure can be expressed as follows [18], [19]:

$$r = |r| \exp(i\varphi_r) = \frac{r_{12} + r_{12}r_{23}r_{34}\exp(2ikd_3) + [r_{23} + r_{34}\exp(2ik_{3z}d_3)]\exp(2ik_{2z}d_2)}{1 + r_{23}r_{34}\exp(2ik_{3z}d_3) + r_{12}[r_{23} + r_{34}\exp(2ik_{3z}d_3)]\exp(2ik_{2z}d_2)} \quad (6)$$

where $\varphi_r = \text{Im}(\ln r)$, $r_{12} = (k_{1z} - k_{2z})/(k_{1z} + k_{2z})$, $r_{23} = (k_{2z} - k_{3z})/(k_{2z} + k_{3z})$, $r_{34} = (k_{3z} - k_{4z})/(k_{3z} + k_{4z})$, $k_{zm} = \sqrt{k_m^2 - k_x^2}$ is the z-component of wave vector in medium m ($m = 1, 2, 3$), k_m is the wave number of light in medium m , $k_x = k_1 \sin \theta$, θ is the incident angle of the terahertz wave, $k_m = n_m k_0$, n_m is the refractive index of medium m , n_1 is the refractive index of the silicon prism, $n_1 = 3.42$, n_2 is the refractive index of the graphene, n_3 is the refractive index of the SiO₂, $n_3 = 1.975$, k_0 is the propagation constant in a vacuum, $k_0 = 2\pi/\lambda$, λ is the incident wavelength, d_2 is the thickness of the graphene, $d_2 = 0.33$ nm, and d_3 is the thickness of the SiO₂.

Based on the stationary phase theory, the Goos–Hänchen shift (S) of the reflected terahertz wave can be written as [20]

$$S = -\frac{\lambda}{2\pi n_1} \cdot \frac{d\varphi_r}{d\theta}. \quad (7)$$

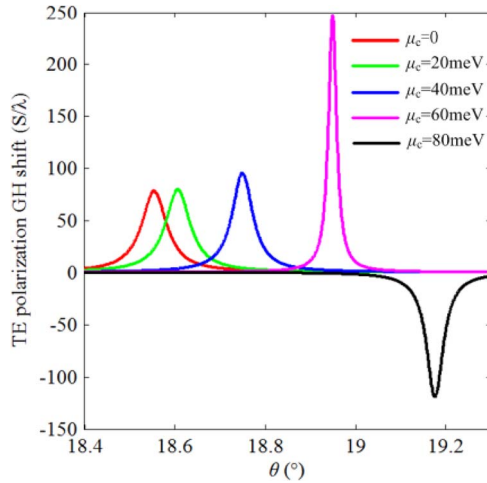


Fig. 5. Dependence of the Goos–Hänchen shifts on the incident angle with different chemical potential.

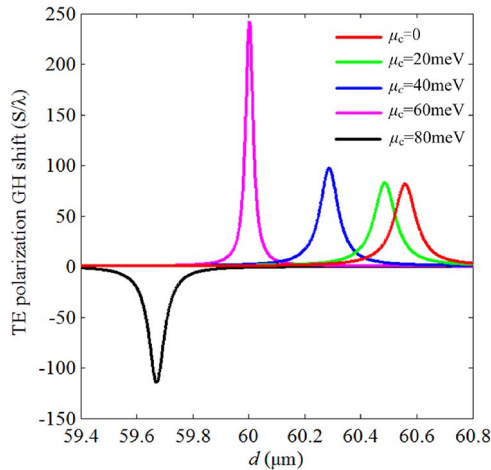


Fig. 6. Goos–Hänchen shift versus SiO_2 thickness with different chemical potential at a fixed incidence angle.

3. Results Analysis and Discussion

In this article, the incident terahertz wavelength is set to be $\lambda = 200 \mu\text{m}$ (i.e., $f = 1.5 \text{ THz}$). The numerical results for the Goos–Hänchen shift of the proposed structure are shown in Fig. 5 as the terahertz wave incident angle (θ) varies from 18.4° to 19.25° with different chemical potential. From the figure, one can see easily that the maximum difference values of the Goos–Hänchen shifts (i.e., The Goos–Hänchen shift is about 250 times of the incident terahertz wavelength.) between the chemical potential $\mu_c = 0 \text{ meV}$ and $\mu_c = 60 \text{ meV}$ are achieved at $\theta = 18.949^\circ$ for incident terahertz wave. As the chemical potential increases to be 80 meV , the Goos–Hänchen shift exhibits a large negative value. The negative Goos–Hänchen shifts are caused by the backward energy flux flow of the evanescent wave or leaky surface wave [21], [22]. When the thickness of the SiO_2 is changed from $59.4 \mu\text{m}$ to $60.8 \mu\text{m}$, while maintaining other structure parameters the same as the design in Fig. 5, the Goos–Hänchen shifts are calculated in Fig. 6. From Fig. 6, one can see that the Goos–Hänchen shift of the reflected terahertz wave is largest when the SiO_2 thickness is of $60 \mu\text{m}$ with chemical potential

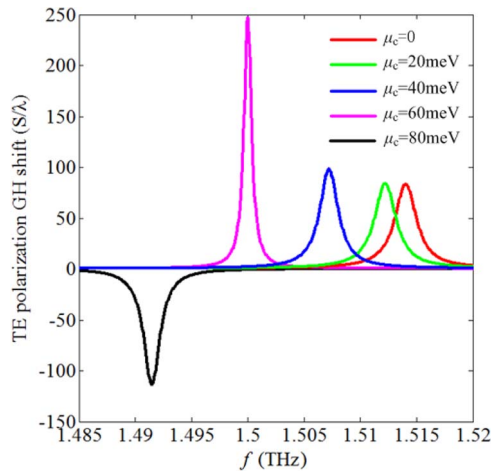


Fig. 7. Dependence of the Goos–Hänchen shifts on the incident frequency with different chemical potential.

$\mu_c = 60$ meV. Moreover, with increasing the chemical potential, we can further find that the Goos–Hänchen shift of the reflected terahertz wave can crossover from positive to negative values. Fig. 7 shows Goos–Hänchen shift curves from the (1)–(9) at the parameters of $\theta = 18.949^\circ$, $d_2 = 0.33$ nm (a single layer graphene sheet) and $d_3 = 60$ μm , when the incident frequency varies from 1.485 THz to 1.52 THz. From the figure, it can be noted that the maximum difference values of the Goos–Hänchen shifts between the chemical potential $\mu_c = 0$ meV and $\mu_c = 60$ meV are achieved at 1.5 THz (i.e., $\lambda = 200$ μm) for incident terahertz wave.

Here, we employ the proposed configuration (see Fig. 1) to design a terahertz wave switch based on a giant tunable Goos–Hänchen shift by changing the external controlling electric field. From Figs. 6 and 7, it is clearly seen that the Goos–Hänchen shift is almost zero without external applied electric field (i.e., $\mu_c = 0$). At this time, the fixed terahertz detector can detect the reflected terahertz wave, and we define the terahertz wave switch as the “on” state. For $\mu_c = 60$ meV, a giant lateral Goos–Hänchen shift of reflected terahertz wave takes place (Here, the Goos–Hänchen shift is about 250 times of the incident terahertz wavelength, i.e., 50 mm.). But in general, the diameter of the incident terahertz wave beam waist is about 5 mm. Therefore, at this moment, the fixed terahertz detector can not detect the reflected terahertz wave beam. Hence, we take the terahertz wave switch as “off” state. Our theoretical analysis shows that the Goos–Hänchen shift of reflected terahertz wave in prism/graphene is strongly chemical potential dependent. The study of lateral Goos–Hänchen shift happened on the prism/graphene structure make sense for e.g., terahertz wave switch application.

To summarize, we proposed a prism/graphene configuration to control the Goos–Hänchen shift of the reflected terahertz wave beam by applying an external voltage. It is found that the lateral Goos–Hänchen shifts of the reflected terahertz wave beam can be easily controlled by adjusting the intensity of the external applied electric field. The Goos–Hänchen shifts may become negative and positive with increasing the external controlling electric field under different conditions. Moreover, through the suitable adjustment of the external controlling electric field, one may realize a giant Goos–Hänchen shift. Using this scheme, the lateral Goos–Hänchen shift at the fixed incident angle can be enhanced (positive or negative) under the suitable conditions on the external applied electric field, without changing the proposed configuration.

Acknowledgement

The authors are grateful to J. Yao for providing useful information and helpful suggestions.

References

- [1] B. Schuklin and X. Zhang, "Active balance in free-space electro-optic detection of terahertz waves," *J. Lightw. Technol.*, vol. 27, no. 17, pp. 3773–3776, Sep. 2009.
- [2] M. Tonouchi, "Cutting-edge terahertz technology," *Nature Photon.*, vol. 1, pp. 97–105, 2007.
- [3] Z. Taylor *et al.*, "Reflective terahertz imaging of porcine skin burns," *Opt. Lett.*, vol. 33, no. 11, pp. 1258–1260, Jun. 2008.
- [4] L. Ren *et al.*, "Terahertz and infrared spectroscopy of gated large-area graphene," *Nano Lett.*, vol. 12, no. 7, pp. 3711–3715, 2012.
- [5] T. Nagatsuma *et al.*, "Terahertz wireless communications based on photonics technologies," *Opt. Exp.*, vol. 21, no. 20, pp. 23 736–23 747, Oct. 2013.
- [6] J. Li, "Terahertz modulator using photonic crystals," *Opt. Commun.*, vol. 269, no. 1, pp. 98–101, Jan. 2007.
- [7] C. Chen, C. Pan, C. Hsieh, and Y. Lin, "Liquid-crystal-based terahertz tunable Lyot filter," *Appl. Phys. Lett.*, vol. 88, no. 10, Mar. 2006, Art. ID. 101107.
- [8] T. Chen *et al.*, "A metamaterial solid-state terahertz phase modulator," *Nature Photon.*, vol. 3, pp. 141–151, 2009.
- [9] J. Shu *et al.*, "High-contrast terahertz modulator based on extraordinary transmission through a ring aperture," *Opt. Exp.*, vol. 19, no. 27, pp. 26 666–26 671, Dec. 2011.
- [10] F. Goos and H. Hänchen, "Ein neuer und fundamentaler versuch zur totalreflexion," *Ann. Phys.*, vol. 436, no. 7/8, pp. 333–346, 1947.
- [11] W. Löffler *et al.*, "Polarization-dependent Goos–Hänchen shift at a graded dielectric interface," *Opt. Commun.*, vol. 283, no. 18, pp. 3367–3370, Sep. 2010.
- [12] J. C. Martinez and M. B. A. Jallil, "Theory of giant Faraday rotation and Goos–Hänchen shift in graphene," *Europhys. Lett.*, vol. 96, no. 2, p. 27008, Oct. 2011.
- [13] M. Sharma and S. Ghosh, "Electron transport and Goos–Hänchen shift in graphene with electric and magnetic barriers," *J. Phys., Condensed Matter*, vol. 23, no. 5, Feb. 2011, Art. ID. 055501.
- [14] Q. Li, B. Zhang, and J. Shen, "Goos–Hänchen shifts of reflected terahertz wave on a COC-air interface," *Opt. Exp.*, vol. 21, no. 5, pp. 6480–6487, Mar. 2013.
- [15] V. Gausynin, S. Sharapov, and J. Carbotte, "Magneto-optical conductivity in graphene," *J. Phy. Condens Matter*, vol. 19, no. 2, Jan. 2007, Art. ID. 026222.
- [16] R. Alaei, M. Farhat, C. Rockstuhl, and F. Lederer, "A perfect absorber made of a graphene micro-ribbon metamaterial," *Opt. Exp.*, vol. 20, no. 27, pp. 28 017–28 024, Dec. 2012.
- [17] G. Lovat, "Equivalent circuit for electromagnetic interaction and transmission through graphene sheets," *IEEE Trans. Electromagn. Compat.*, vol. 54, no. 1, pp. 101–109, Feb. 2012.
- [18] L. Chen *et al.*, "Observation of large positive and negative lateral shifts of a reflected beam from symmetrical metal-cladding waveguides," *Opt. Lett.*, vol. 32, no. 11, pp. 1432–1434, Jun. 2007.
- [19] M. Liu, Q. Zhao, F. Zhu, F. Yang, and S. Zhang, "Net lateral shift of reflected beam in prism-waveguide coupling system due to guided wave resonance," *Opt. Commun.*, vol. 310, 75–79, Jan. 2014.
- [20] J. D. Jackson, *Classical Electrodynamics*, 3rd ed. New York, NY, USA: Wiley, 1999, pp. 300–350.
- [21] F. Schreier, M. Schmitz, and O. Bryngdahl, "Beam displacement at diffractive structures under resonance conditions," *Opt. Lett.*, vol. 23, no. 8, pp. 576–578, Apr. 1998.
- [22] H. Lai, C. Kwok, Y. Loo, and B. Xu, "Energy-flux pattern in the Goos–Hänchen effect," *Phys. Rev. E*, vol. 62, no. 5, pp. 7330–7339, Apr. 2000.